

Electrophobic Scalar Boson and Muonic Puzzles

Yu-Sheng Liu,* David McKeen,† and Gerald A. Miller‡

Department of Physics, University of Washington, Seattle, Washington 98195-1560, U.S.A.

(Dated: September 13, 2016)

A new scalar boson which couples to the muon and proton can simultaneously solve the proton radius puzzle and the muon anomalous magnetic moment discrepancy. Using a variety of measurements, we constrain the mass of this scalar and its couplings to the electron, muon, neutron, and proton. Making no assumptions about the underlying model, these constraints and the requirement that it solve both problems limit the mass of the scalar to between about 100 keV and 100 MeV. We identify two unexplored regions in the coupling constant-mass plane. Potential future experiments and their implications for theories with mass-weighted lepton couplings are discussed.

Recent measurements of the proton charge radius using the Lamb shift in muonic hydrogen are troublingly discrepant with values extracted from hydrogen spectroscopy and electron-proton scattering. Presently, the value from muonic hydrogen is 0.84087(39) fm [1, 2] while the CODATA average of data from hydrogen spectroscopy and e - p scattering yields 0.8751(61) fm [3]; these differ at more than 5σ . Although the discrepancy may arise from subtle lepton-nucleon non-perturbative effects within the standard model or experimental uncertainties [4, 5], it could also be a signal of new physics involving a violation of lepton universality.

The muon anomalous magnetic moment provides another potential signal of new physics. The BNL [6] measurement differs from the standard model prediction by at least three standard deviations, $\Delta a_\mu = a_\mu^{\text{exp}} - a_\mu^{\text{th}} = 287(80) \times 10^{-11}$ [7, 8].

A new scalar boson, ϕ , that couples to the muon and proton could explain both the proton radius and $(g-2)_\mu$ puzzles [9]. We investigate the couplings of this boson to standard model fermions, f , which appear as terms in the Lagrangian, $\mathcal{L} \supset e\epsilon_f\phi\bar{f}f$, where $\epsilon_f = g_f/e$ and e is the electric charge of the proton. Other authors have pursued this basic idea, but made further assumptions relating the couplings to different species; e.g. in [9], ϵ_p is taken equal to ϵ_μ and in [10], mass-weighted couplings are assumed. References [9] and [10] both neglect ϵ_n . We make no *a priori* assumptions regarding signs or magnitudes of the coupling constants. The Lamb shift in muonic hydrogen fixes ϵ_μ and ϵ_p to have the same sign which, we take to be positive. ϵ_e and ϵ_n are allowed to have either sign.

We focus on the scalar boson possibility because scalar exchange produces no hyperfine interaction, in accord with observation [1, 2]. The emission of possible new vector particles becomes copious at high energies, and in the absence of an ultraviolet completion, is ruled out [11].

Scalar boson exchange can account for both the proton radius puzzle and the $(g-2)_\mu$ discrepancy [9]. The shift of the lepton ($\ell = \mu, e$) muon's magnetic moment due to

one-loop ϕ exchange is given by [12]

$$\Delta a_\ell = \frac{\alpha\epsilon_\ell^2}{2\pi} \int_0^1 dz \frac{(1-z)^2(1+z)}{(1-z)^2 + (m_\phi/m_\ell)^2 z}. \quad (1)$$

Scalar exchange between fermions f_1 and f_2 leads to a Yukawa potential, $V(r) = -\epsilon_{f_1}\epsilon_{f_2}\alpha e^{-m_\phi r}/r$. In atomic systems, this leads to an additional contribution to the Lamb shift in the 2S-2P transition. For an (electronic or muonic) atom, of A and Z this shift is given by [13]

$$\delta E_L^{\ell N} = -\frac{\alpha}{2a_{\ell N}} \epsilon_\ell [Z\epsilon_p + (A-Z)\epsilon_n] f(a_{\ell N} m_\phi) \quad (2)$$

where $f(x) = x^2/(1+x)^4$ [9, 14], with $a_{\ell N} = (Z\alpha m_{\ell N})^{-1}$ the Bohr radius and $m_{\ell N}$ is the reduced mass of the lepton-nucleus system. Throughout this paper we set

$$\Delta a_\mu = 287(80) \times 10^{-11}, \quad \delta E_L^{\mu H} = -0.307(56) \text{ meV} \quad (3)$$

within two standard deviations. This value of $\delta E_L^{\mu H}$, is the same as the energy shift caused by using the different values of the proton radius [1–3, 15] to explain the two discrepancies. This allows us to determine both ϵ_p and ϵ_μ as functions of m_ϕ . The unshaded regions in Figs. 1 and 3 show the values of ϵ_p and ϵ_μ , as functions of the scalar's mass, that lead to the values of Δa_μ and $\delta E_L^{\mu H}$ in Eq. (3).

We study several observables sensitive to the couplings of the scalar to neutrons, ϵ_n , and protons, ϵ_p to obtain new bounds on m_ϕ .

- Low energy scattering of neutrons on ^{208}Pb has been used to constrain light force carriers coupled to nucleons [16] assuming a coupling of a scalar to nucleons of g_N . Using the replacement

$$\frac{g_N^2}{e^2} \rightarrow \frac{A-Z}{A} \epsilon_n^2 + \frac{Z}{A} \epsilon_p \epsilon_n \quad (4)$$

for scattering on a nucleus with atomic mass A and atomic number Z , we separately constrain the coupling of a scalar to protons and neutrons.

- The known NN charge-independence breaking scattering length difference, defined as $\Delta a = \bar{a} - a_{np}$,

* mestelqre@gmail.com

† dmckeen@uw.edu

‡ miller@phys.washington.edu

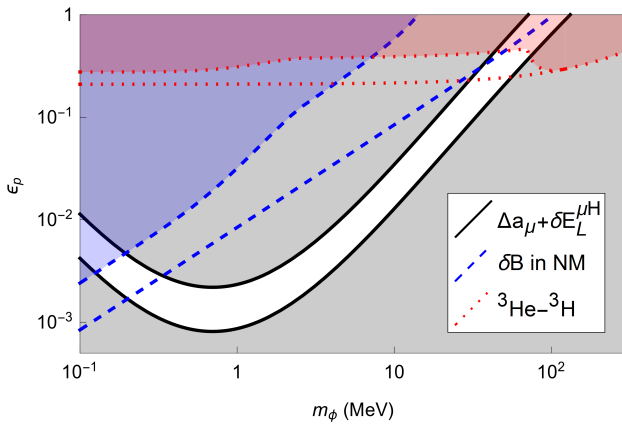


FIG. 1. (Color online) Exclusion (shaded regions) plot for ϵ_p . The region between the black lines is allowed via Eqs. 1-3. The dashed blue and dotted red lines represent the constraints from nucleon binding energy in infinite nuclear matter and the ${}^3\text{He}-{}^3\text{H}$ binding energy difference; isolated lines are derived using $\epsilon_n = 0$ and the shaded regions are excluded using the constraint on ϵ_n/ϵ_p in Fig. 2.

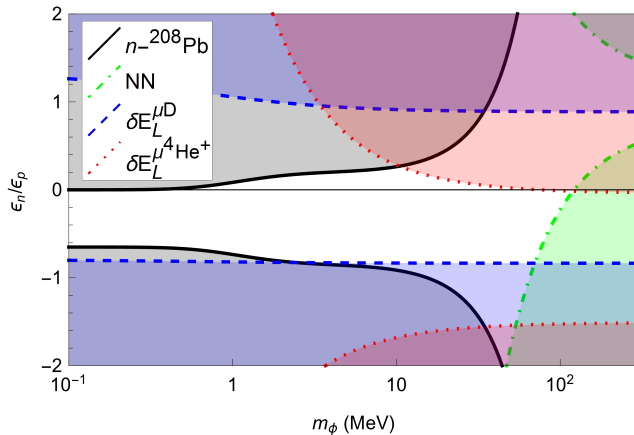


FIG. 2. (Color online) Exclusion (shaded regions) plot for ϵ_n/ϵ_p . The black, dashed blue, dotted red, and dotted green lines correspond to the constraints from $n-{}^{208}\text{Pb}$ scattering, μD Lamb shift, $\mu^4\text{He}^+$ Lamb shift, and NN scattering length difference.

with $\bar{a} \equiv (a_{pp} + a_{nn})/2$. The measured value $\Delta a^{\text{exp}} = 5.64(60)$ fm [17] is reproduced by a variety of known effects: $\Delta a^{\text{th}} = 5.6(5)$ fm [18]. The existence of the scalar boson gives an additional contribution

$$\Delta a_\phi = \bar{a} a_{np} M \int_0^\infty \Delta V \bar{u} u_{np} dr, \quad (5)$$

where M is the average of the nucleon mass; $\Delta V = -\frac{1}{2}\alpha(\epsilon_p - \epsilon_n)^2 e^{-m_\phi r}/r$; $u(r)$ is the zero energy 1S_0 wave function, normalized so that $u(r) \rightarrow (1 - r/a)$ as $r \rightarrow \infty$. To avoid spoiling the agreement with experiment Δa_ϕ cannot be greater than 1.6 fm (using 2 S.D. as allowable).

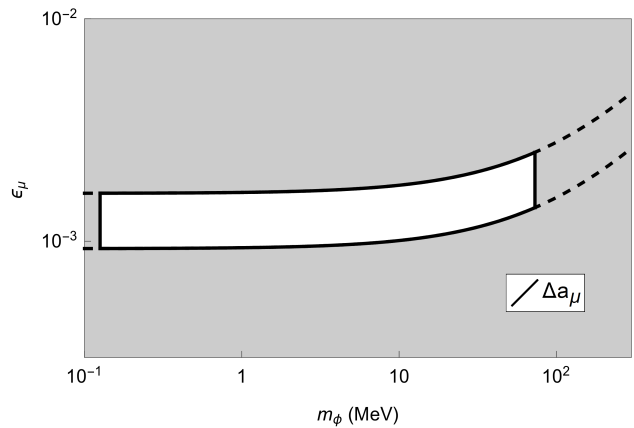


FIG. 3. Exclusion (shaded region) plot for ϵ_μ . The region between the solid and dashed lines are obtained using $(g-2)_\mu$ Eq. (1) with 2 S.D.. The restrictions on the values of m_ϕ in Fig. 1 cause the region between the dashed lines to be excluded.

- The volume term in the semi-empirical mass formula gives the binding energy per nucleon in $N = Z$ infinite nuclear matter. Scalar boson exchange provides an additional contribution. Using the Hartree approximation, which is accurate if $m_\phi < 100$ MeV [19, 20], we find the average change in nucleon binding energy in infinite nuclear matter to be $(\delta B_p + \delta B_n)/2 = (g_p + g_n)^2 \rho / 4m_\phi^2$ which (with $\rho \approx 0.08 \text{ fm}^{-3}$) must not exceed 1 MeV to avoid problems with existing understanding of nuclear physics.
- The difference in the binding energies of ${}^3\text{He}$ and ${}^3\text{H}$ of 763.76 keV is nicely explained by the effect of Coulomb interaction (693 keV) and charge asymmetry of nuclear forces (about 68 keV) [21–25]. The contribution to the binding energy difference from the scalar boson can be estimated by using the nuclear wave function extracted from elastic electron-nuclei scattering [22, 26–28]. We set constraints by requiring that this contribution not exceed 30 keV to maintain the agreement between theory and experiment.
- We use the preliminary results on the Lamb shifts in muonic deuterium and muonic ${}^4\text{He}$. For μD a discrepancy similar to that of μH between the charge radius extracted via the Lamb shift of μD , $r_D^\mu = 2.1272(12)$ fm [29] and the CODATA average from electronic measurements, $r_D = 2.1213(25)$ fm [3], exists. This could be also be explained by a scalar coupled to muons that results in a change to the Lamb shift of $\delta E_L^{\mu\text{D}} = -0.368(78)$ meV [15, 30]. The similarity of this shift to the one required in μH constrains the coupling of ϕ to the neutron. For $\mu^4\text{He}$, the radii extracted from the muonic Lamb shift measurement,

$r_{4\text{He}}^\mu = 1.677(1)$ fm [31], and elastic electron scattering, $r_{4\text{He}} = 1.681(4)$ fm [32], require the change in the Lamb shift due to ϕ exchange to be compatible with zero, $\delta E_L^{\mu^4\text{He}^+} = -1.4(1.5)$ meV [15]. Since these results are preliminary, we draw constraints at the 3σ level. Using the ratio of nuclear to hydrogen Lamb shifts for D and He via Eq. (2) allows us to obtain ϵ_n/ϵ_p independently of the value of ϵ_μ and ϵ_p . We expect that publication of the D and ^4He data would provide constraints at the 2σ level, thereby narrowing the allowed region by a factor of about $2/3$ and changing details of the borders of the allowed regions.

Using these observables (as constrained by Eqs. (1-3)) we limit the ratio of the coupling of ϕ to neutrons and protons, ϵ_n/ϵ_p , as shown in Fig. 2. If the couplings to neutron and proton are of the same sign, these constraints are quite strong, driven by the neutron- ^{208}Pb scattering limits for $m_\phi \lesssim 10$ MeV and the $\mu^4\text{He}$ measurement for larger masses. If the couplings are of opposite sign, they interfere destructively, masking the effects of the ϕ and substantially weakening the limits on the magnitudes of ϵ_n, ϵ_p .

For a given value of ϵ_n/ϵ_p , we use the shift of the binding energy in $N = Z$ nuclear matter and the difference in binding energies of ^3H and ^3He to constrain ϵ_p . We show these bounds in Fig. 1, varying ϵ_n/ϵ_p over its allowed range as a function of m_ϕ . These measurements limit the mass of the scalar that simultaneously explains the proton radius and $(g-2)_\mu$ discrepancies to $100 \text{ keV} \lesssim m_\phi \lesssim 100 \text{ MeV}$. These upper and lower limits on the allowed value of m_ϕ are also indicated on the plot of the required values of ϵ_μ in Fig. 3.

We now explore the coupling of the scalar to electrons, which is of particular experimental importance because electrons are readily produced and comparatively simple to understand. The limits on the coupling ϵ_e are similar to many that have been placed on the dark photon in recent years (see, e.g. [34]). Below, we describe the experimental quantities used to derive limits on the electron-scalar coupling.

Scalar exchange shifts the anomalous magnetic moment of the electron; see Eq. (1). As emphasized in Ref. [35], the measurement of $(g-2)_e$ is currently used to extract the fine structure constant. A constraint on ϵ_e can therefore be derived by comparing the inferred value of α with a value obtained from a measurement that isn't sensitive to the contribution of the scalar boson. We use the precision study of ^{87}Rb [36]. Requiring that these two measurements agree implies that $\Delta a_e < 1.5 \times 10^{-12}$ (2 S.D.).

Bhabha scattering, $e^+e^- \rightarrow e^+e^-$, can be used to search for the scalar boson by looking for a resonance due to ϕ exchange. Motivated by earlier results from heavy-ion collisions near the Coulomb barrier, a GSI group [37] used a clean time-stable monoenergetic positron beam incident on a metallic Be foil. No resonances were observed

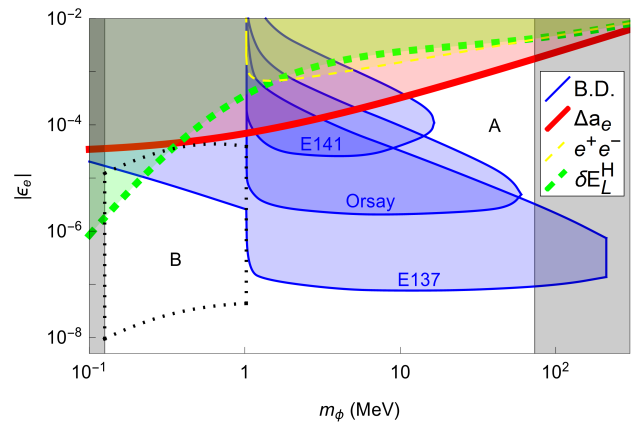


FIG. 4. (Color online) Exclusion (shaded regions) plot for ϵ_e . The thick red, thin blue, thin dashed yellow, and thick dashed green lines correspond to the constraints from electron anomalous magnetic moment $(g-2)_e$, beam dump experiments, Bhabha scattering, and the Lamb shift of hydrogen. The region between the two vertical gray regions are allowed using the scalar mass range from Fig. 1. Regions A and B could be covered by the proposed experiments in: [33], [10] and the study [34].

at the 97% C.L. within the experimental sensitivity of 0.5 b eV/sr (c.m.) for the energy-integrated differential cross section. Given the small value of ϵ_e the only relevant process is the s -channel exchange of a ϕ boson, which was not observed. The experiment limits $|\epsilon_e|$ as shown in Fig. 4.

Beam dump experiments have long been used to search for light, weakly coupled particles that decay to leptons or photons [33, 34, 38]. If coupled to electrons, ϕ bosons could be produced in such experiments and decay to e^+e^- or $\gamma\gamma$ pairs depending on its mass. The production cross section for the scalar boson, not in the current literature, is discussed in a longer paper [39] to be presented later. Previous work [33] simplified the evaluation of this cross section by using the Weizsacker-Williams (WW) approximation, by making further approximations to the phase space integral, assuming that the mass of the new particle is much greater than electron mass, and can't be used if $m_\phi < 2m_e$. Our numerical evaluations [39] do not use these assumptions and thereby allow us to cover the entire mass range shown in Fig. 4. In particular, we find that the approximations of [33] have significant errors for $m_\phi > 10$ MeV. Our analysis uses data from the electron beam dump experiments E137 [38], E141 [40], and Orsay [41].

In addition to muonic atoms, scalar exchange will affect the Lamb shift in ordinary electronic atoms. To set limits on the coupling, following [42-44], we require that the change to the Lamb shift in hydrogen is $\delta E_L^H < 14 \text{ kHz}$ [45](2 S.D.).

In Fig. 4, we present the constraints on the coupling to electrons, ϵ_e , as a function of m_ϕ from these observables. In addition we indicate (via two dashed vertical lines) the

allowed mass range for ϕ , taken from Fig. 1.

We label two allowed regions in the (m_ϕ, ϵ_e) plane in Fig. 4: A, where $10 \text{ MeV} \lesssim m_\phi \lesssim 70 \text{ MeV}$, $10^{-6} \lesssim \epsilon_e \lesssim 10^{-3}$, and B, where $100 \text{ keV} \lesssim m_\phi \lesssim 1 \text{ MeV}$, $10^{-8} \lesssim \epsilon_e \lesssim 10^{-5}$. There are a number of planned electron scattering experiments that will be sensitive to scalars with parameters in Region A, such as, e.g., APEX [46], HPS [47], DarkLight [48], VEPP-3 [49], and MAMI or MESA [50]. As studied in Ref. [10], region B can be probed by looking for scalars produced in the nuclear de-excitation of an excited state of ^{16}O . We have translated this region of couplings $10^{-11} \leq \epsilon_p \epsilon_e \leq 10^{-7}$ from Ref. [10] to show on our plot by taking $\epsilon_p \rightarrow \epsilon_p + \epsilon_n$, using ϵ_n/ϵ_p from Fig. 2 and fixing ϵ_p according to (3).

We do not show limits derived from stellar cooling that are sensitive to $m_\phi \lesssim 200 \text{ keV}$ [51] since the lower bound on the mass is similar to the one we have derived. Additionally, we note that constraints from cooling of supernovae do not appear in Fig. 4. This is because the required value of g_p is always large enough to keep any scalars produced trapped in supernova, rendering cooling considerations moot [52]. The effects of this scalar boson may have cosmological consequences, beyond the scope of this article.

We summarize the parameter space (see also Table I):

1. The range of allowed m_ϕ is widened from a narrow region around 1 MeV in [9] to the region from about 130 keV to 73 MeV by allowing $\epsilon_p \neq \epsilon_\mu$.
2. We carefully deal with ϵ_n instead of neglecting it. In particular, as seen in Fig. 1, allowing ϵ_n to be of the opposite sign of ϵ_p opens up the parameter space.
3. The constraint on ϵ_e at $m_\phi = 1 \text{ MeV}$ is improved by two orders of magnitude compared with [9] by using electron beam dump experiments.
4. Near the maximum allowed $m_\phi \sim 70 \text{ MeV}$, the allowed couplings are relatively large, $|\epsilon_e| < 1.8 \times 10^{-3}$; $10^{-3} < \epsilon_\mu < 2 \times 10^{-3}$; $\epsilon_p \lesssim 0.4$; $-0.3 \lesssim \epsilon_p \lesssim 0$, providing ample opportunity to test this solution.

Our discussion thus far has been purely phenomenological, with no particular UV completion in mind to relate the couplings of fermions with the same quantum numbers (here the electron and muon). From the model-building point of view, there are motivations that the couplings of ϕ to fermions in the same family are mass-weighted—in particular, for the leptons, $|\epsilon_\mu/\epsilon_e| = (m_\mu/m_e)^n$ with $n \geq 1$. This is because, generally, coupling fermions to new scalars below the electroweak scale leads to large flavor-changing neutral currents (FCNCs) that are very strongly constrained, e.g. in the lepton sector by null searches for $\mu \rightarrow e$ conversion, $\mu \rightarrow 3e$, or $\mu \rightarrow e\gamma$. A phenomenological ansatz for the structure of the ϕ 's couplings to fermions that avoids this problem is that its Yukawa matrix is proportional to that of

the Higgs. This scenario has been termed minimal flavor violation (MFV), see e.g. [53]. In that case, both the Higgs and ϕ couplings are simultaneously diagonalized and new FCNCs are absent. The main phenomenological consequence of this is that ϕ 's coupling to a lepton is proportional to a power of that lepton's mass, $\epsilon_\ell \propto m_\ell^n$ with $n \geq 1$. In the context of a given model, i.e. for fixed n , we can relate Figs. 3 and 4. Region A largely corresponds to $0 < n \lesssim 1$, which, is less well-motivated from a model building perspective. $1 \lesssim n \lesssim 2$ is well-motivated and fits into Region B. To obtain $\epsilon_e \lesssim 10^{-7}$, $n \gtrsim 2$ is required. All of the allowed values of ϵ_e are smaller than the required value of ϵ_μ , thus the name electrophobic scalar boson is applicable.

Building a complete model, valid at high energy scales, leading to interactions at low energies is not our purpose. However, we outline one simple possibility. In the lepton sector, couplings to ϕ could arise through mixing obtained via a lepton-specific two Higgs doublet model, which would automatically yield MFV [54]. In the quark sector, coupling to a light boson via mixing with a Higgs is very tightly constrained by null results in $K \rightarrow \pi$ and B meson decays (see, e.g., Ref. [55]) decays. However, as in Ref. [56], heavy vector-like quarks that couple to ϕ and mix primarily with right-handed quarks of the first generation due to a family symmetry are a possibility. The coupling strength of ϕ to u and d quarks could differ leading to different couplings to neutrons and protons. If, e.g., $g_d/g_u \sim -0.8$ then $g_n/g_p \sim -0.5$, which, as we see in Fig. 2, is comparatively less constrained.

The existence of a scalar boson that couples to muons and protons accounts for the proton radius puzzle and the present discrepancy in the muon anomalous magnetic moment. Many previous experiments could have detected this particle, but none did. Nevertheless, regions A and B in Fig. 4 remain open for discovery.

For masses m_ϕ near the allowable maximum, the value of ϵ_p can be as large as about 0.4. Such a coupling could be probed with proton experiments, such as threshold ϕ production in pp interactions. Proton or muon beam dump experiments could also be used [57]. Can one increase the accuracy of the neutron-nucleus experiments? For experiments involving muons, one might think of using muon beam dump experiments, such as the COMPASS experiment as proposed in [58]. The MUSE experiment [59] plans to measure μ^\pm and e^\pm -p elastic scattering at low energies. Our hypothesis regarding the ϕ leads to a prediction for the MUSE experiment even though its direct effect on the scattering will be very small [60]: the MUSE experiment will observe the same 'large' value of the proton radius for all of the probes. Another possibility is to study the spectroscopy of muonium (the bound state of e^- and μ^+) or true muonium (the bound state of μ^- and μ^+). Perhaps the best way to test the existence of this particle would be an improved measurement of the muon anomalous magnetic moment [61]. The existence of a particle with such a limited role may seem improbable, considering the present state of knowledge.

TABLE I. Allowed coupling with various scalar mass: numbers in the parentheses are 1 S.D..

m_ϕ (MeV)	$ \epsilon_e $	ϵ_μ	ϵ_p	ϵ_n
0.13	$< 2.0 \times 10^{-6}$	$1.29(18) \times 10^{-3}$	3.0×10^{-3}	-2.0×10^{-3} to 2.8×10^{-7}
1	$< 2.6 \times 10^{-6}$	$1.30(18) \times 10^{-3}$	$1.60(37) \times 10^{-3}$	-1.7×10^{-3} to 2.0×10^{-4}
10	$< 7.6 \times 10^{-8}$	$1.40(20) \times 10^{-3}$	$2.37(54) \times 10^{-2}$	-2.9×10^{-2} to 9.1×10^{-3}
73	$< 9.1 \times 10^{-8}$ 3.3×10^{-6} to 1.8×10^{-3}	$1.96(27) \times 10^{-3}$	0.39	-0.29 to 5.6×10^{-4}

However, such an existence is not ruled out.

ACKNOWLEDGMENTS.

We thank M. Barton-Rowledge, J. Detwiler, R. Machleidt, S. Reddy, and M. J. Savage for invaluable discus-

sions and suggestions. The work of G. A. M. and Y.-S. L. was supported by the U. S. Department of Energy Office of Science, Office of Nuclear Physics under Award Number DE-FG02-97ER-41014. The work of D. M. was supported by the U.S. Department of Energy under Grant No. DE-FG02-96ER-40956.

-
- [1] R. Pohl *et al.*, Nature **466**, 213 (2010).
[2] A. Antognini *et al.*, Science **339**, 417 (2013).
[3] P. J. Mohr, D. B. Newell, and B. N. Taylor, (2015), arXiv:1507.07956.
[4] R. Pohl, R. Gilman, G. A. Miller, and K. Pachucki, Ann. Rev. Nucl. Part. Sci. **63**, 175 (2013), arXiv:1301.0905 [physics.atom-ph].
[5] C. E. Carlson, Prog. Part. Nucl. Phys. **82**, 59 (2015), arXiv:1502.05314 [hep-ph].
[6] T. Blum, A. Denig, I. Logashenko, E. de Rafael, B. Lee Roberts, T. Teubner, and G. Venanzoni, (2013), arXiv:1311.2198 [hep-ph].
[7] M. Davier, A. Hoecker, B. Malaescu, and Z. Zhang, Eur. Phys. J. **C71**, 1515 (2011), [Erratum: Eur. Phys. J.C72,1874(2012)], arXiv:1010.4180 [hep-ph].
[8] K. Hagiwara, R. Liao, A. D. Martin, D. Nomura, and T. Teubner, J. Phys. **G38**, 085003 (2011), arXiv:1105.3149 [hep-ph].
[9] D. Tucker-Smith and I. Yavin, Phys. Rev. **D83**, 101702 (2011), arXiv:1011.4922 [hep-ph].
[10] E. Izaguirre, G. Krnjaic, and M. Pospelov, Phys. Lett. **B740**, 61 (2015), arXiv:1405.4864 [hep-ph].
[11] S. G. Karshenboim, D. McKeen, and M. Pospelov, Phys. Rev. **D90**, 073004 (2014), [Addendum: Phys. Rev.D90,no.7,079905(2014)], arXiv:1401.6154 [hep-ph].
[12] R. Jackiw and S. Weinberg, Phys. Rev. **D5**, 2396 (1972).
[13] G. A. Miller, Phys. Rev. **C91**, 055204 (2015), arXiv:1501.01036 [nucl-th].
[14] V. Barger, C.-W. Chiang, W.-Y. Keung, and D. Marfatia, Phys. Rev. Lett. **106**, 153001 (2011), arXiv:1011.3519 [hep-ph].
[15] A. Antognini *et al.*, *Proceedings, 21st International Conference on Few-Body Problems in Physics (FB21)*, EPJ Web Conf. **113**, 01006 (2016), arXiv:1509.03235 [physics.atom-ph].
[16] H. Leeb and J. Schmiedmayer, Phys. Rev. Lett. **68**, 1472 (1992).
[17] R. Machleidt and I. Slaus, J. Phys. **G27**, R69 (2001), arXiv:nucl-th/0101056 [nucl-th].
[18] T. E. O. Ericson and G. A. Miller, *Proceedings, 10th International Conference on Few Body Problems in Physics (Few Body X)*, Phys. Lett. **B132**, 32 (1983), [Conf. Proc.C830821V2,107(1983)].
[19] R. D. Mattuck, *A Guide to Feynman Diagrams in the Many Body Problem (Second Edition)* (1976).
[20] Discussion with Sanjay Reddy and Martin J. Savage.
[21] J. L. Friar, Nucl. Phys. **A156**, 43 (1970).
[22] J. L. Friar and B. F. Gibson, Phys. Rev. **C18**, 908 (1978).
[23] S. A. Coon and R. C. Barrett, Phys. Rev. **C36**, 2189 (1987).
[24] G. A. Miller, B. M. K. Nefkens, and I. Slaus, Phys. Rept. **194**, 1 (1990).
[25] R. B. Wiringa, S. Pastore, S. C. Pieper, and G. A. Miller, Phys. Rev. **C88**, 044333 (2013), arXiv:1308.5670 [nucl-th].
[26] I. Sick, Prog. Part. Nucl. Phys. **47**, 245 (2001), arXiv:nucl-ex/0208009 [nucl-ex].
[27] F. P. Juster *et al.*, Phys. Rev. Lett. **55**, 2261 (1985).
[28] J. S. McCarthy, I. Sick, and R. R. Whitney, Phys. Rev. **C15**, 1396 (1977).
[29] Reported at Fundamental Constants Meeting 2015 by Randolph Pohl for the CREMA collaboration.
[30] J. J. Krauth, M. Diepold, B. Franke, A. Antognini, F. Kottmann, and R. Pohl, Annals Phys. **366**, 168 (2016), arXiv:1506.01298 [physics.atom-ph].
[31] Reported at NuPECC 2015 by Aldo Antognini for the CREMA collaboration.
[32] I. Sick, Phys. Rev. **C90**, 064002 (2014), arXiv:1412.2603 [nucl-ex].
[33] J. D. Bjorken, R. Essig, P. Schuster, and N. Toro, Phys. Rev. **D80**, 075018 (2009), arXiv:0906.0580 [hep-ph].
[34] R. Essig *et al.*, *Community Summer Study 2013: Snowmass on the Mississippi (CSS2013) Minneapolis, MN, USA, July 29-August 6, 2013*, (2013), arXiv:1311.0029 [hep-ph].
[35] M. Pospelov, Phys. Rev. **D80**, 095002 (2009), arXiv:0811.1030 [hep-ph].
[36] R. Bouchendira, P. Clade, S. Guellati-Khelifa, F. Nez, and F. Biraben, Phys. Rev. Lett. **106**, 080801 (2011),

- arXiv:1012.3627 [physics.atom-ph].
- [37] H. Tsertos, C. Kozhuharov, P. Armbruster, P. Kienle, B. Krusche, and K. Schreckenbach, *Phys. Rev.* **D40**, 1397 (1989).
- [38] J. D. Bjorken, S. Ecklund, W. R. Nelson, A. Abashian, C. Church, B. Lu, L. W. Mo, T. A. Nunamaker, and P. Rassmann, *Phys. Rev.* **D38**, 3375 (1988).
- [39] Y.-S. Liu, D. McKeen, and G. A. Miller, *in preparation*.
- [40] E. M. Riordan *et al.*, *Phys. Rev. Lett.* **59**, 755 (1987).
- [41] M. Davier and H. Nguyen Ngoc, *Phys. Lett.* **B229**, 150 (1989).
- [42] G. A. Miller, A. W. Thomas, J. D. Carroll, and J. Rafelski, *Phys. Rev.* **A84**, 020101 (2011), arXiv:1101.4073 [physics.atom-ph].
- [43] G. A. Miller, A. W. Thomas, and J. D. Carroll, *Phys. Rev.* **C86**, 065201 (2012), arXiv:1207.0549 [nucl-th].
- [44] G. A. Miller, *Phys. Lett.* **B718**, 1078 (2013), arXiv:1209.4667 [nucl-th].
- [45] M. I. Eides, H. Grotch, and V. A. Shelyuto, *Phys. Rept.* **342**, 63 (2001), arXiv:hep-ph/0002158 [hep-ph].
- [46] R. Essig, P. Schuster, N. Toro, and B. Wojtsekhowski, *JHEP* **02**, 009 (2011), arXiv:1001.2557 [hep-ph]; S. Abrahamyan *et al.* (APEX), *Phys. Rev. Lett.* **107**, 191804 (2011), arXiv:1108.2750 [hep-ex].
- [47] M. Battaglieri *et al.*, *Nucl. Instrum. Meth.* **A777**, 91 (2015), arXiv:1406.6115 [physics.ins-det].
- [48] M. Freytsis, G. Ovanessian, and J. Thaler, *JHEP* **01**, 111 (2010), arXiv:0909.2862 [hep-ph]; R. F. Cowan (DarkLight), *Proceedings, Workshop to Explore Physics Opportunities with Intense, Polarized Electron Beams up to 300 MeV*, AIP Conf. Proc. **1563**, 126 (2013).
- [49] B. Wojtsekhowski, D. Nikolenko, and I. Rachek, (2012), arXiv:1207.5089 [hep-ex].
- [50] T. Beranek, H. Merkel, and M. Vanderhaeghen, *Phys. Rev.* **D88**, 015032 (2013), arXiv:1303.2540 [hep-ph].
- [51] H. An, M. Pospelov, and J. Pradler, *Phys. Lett.* **B725**, 190 (2013), arXiv:1302.3884 [hep-ph].
- [52] E. Rrapaj and S. Reddy, (2015), arXiv:1511.09136 [nucl-th].
- [53] V. Cirigliano, B. Grinstein, G. Isidori, and M. B. Wise, *Nucl. Phys.* **B728**, 121 (2005), arXiv:hep-ph/0507001 [hep-ph].
- [54] B. Batell, N. Lange, D. McKeen, M. Pospelov, and A. Ritz, (2016), arXiv:1606.04943 [hep-ph].
- [55] B. Batell, M. Pospelov, and A. Ritz, *Phys. Rev.* **D83**, 054005 (2011), arXiv:0911.4938 [hep-ph].
- [56] P. J. Fox, J. Liu, D. Tucker-Smith, and N. Weiner, *Phys. Rev.* **D84**, 115006 (2011), arXiv:1104.4127 [hep-ph].
- [57] S. Gardner, R. J. Holt, and A. S. Tadepalli, (2015), arXiv:1509.00050 [hep-ph].
- [58] R. Essig, R. Harnik, J. Kaplan, and N. Toro, *Phys. Rev.* **D82**, 113008 (2010), arXiv:1008.0636 [hep-ph].
- [59] R. Gilman *et al.* (MUSE), (2013), arXiv:1303.2160 [nucl-ex].
- [60] Y.-S. Liu and G. A. Miller, *Phys. Rev.* **C92**, 035209 (2015), arXiv:1507.04399 [nucl-th].
- [61] D. W. Hertzog, *Proceedings, Workshop on Flavour changing and conserving processes 2015 (FCCP2015)*, EPJ Web Conf. **118**, 01015 (2016), arXiv:1512.00928 [hep-ex].